

Letter

## Low-temperature self-assembly of copper phthalocyanine nanofibers

Shich-Chang Suen<sup>a</sup>, Wha-Tzong Whang<sup>a,\*</sup>, Fu-Ju Hou<sup>b</sup>, Bau-Tong Dai<sup>b</sup>

<sup>a</sup> Department of Materials Science and Engineering, National Chiao Tung University, 1001 Ta Hsueh Road, Hsinchu 30050, Taiwan, ROC

<sup>b</sup> National Nano Device Laboratories, No. 26, Prosperity Road I, Science-based Industrial Park, Hsinchu, Taiwan, ROC

Received 26 April 2006; received in revised form 29 May 2006; accepted 30 May 2006

Available online 30 June 2006

### Abstract

This paper describes a method for producing 1D organic nanofibers by exploiting intermolecular dispersive forces during the self-assembly of CuPc molecules. The average length of these CuPc nanofibers deposited at 100 °C, a temperature much lower than that required for the synthesis of carbon nanotubes, was ca. 500 nm, with diameters in the range 15–50 nm. XRD analysis of these nanofibers revealed that they possessed an  $\alpha$  phase structure. HRTEM images indicated that the CuPc nanofibers formed through layered stacking of CuPc molecules. These CuPc nanofibers exhibit field emission characteristics (with a turn-on field of 13.6 V/ $\mu$ m) and follow Fowler–Nordheim behavior in a manner similar to that of carbon nanotubes. The stable emission current and relative simplicity of their synthesis suggest a broad range of applications for CuPc nanofibers in nanoscience and nanotechnology.

© 2006 Elsevier B.V. All rights reserved.

PACS: 79.70.+q; 81.07.Nb; 85.35.; 81.16.Dn; 72.80.Le

Keywords: Field emission; Self-assembly (nanofabrication); Organic semiconductors; Nanofibers; Copper Phthalocyanine

### 1. Introduction

One-dimensional (1D) nanostructures of inorganic materials continue to attract a great deal of interest because of their peculiar properties, relative to those of their bulk counterparts, and great potential for application [1–5]. Presently, however, the conditions employed to synthesize such inorganic

nanostructures involve the use of high-temperatures and/or catalysts. Many recent studies have indicated that organic compounds can form 1D nanostructures under mild conditions when intermolecular dispersive forces are exploited in self-assembly processes [6–12]. When biased in a vacuum chamber, most of these nanostructures exhibit excellent field emission characteristics [10–12]. Copper phthalocyanine (CuPc), which has been known for almost a century, is a particularly appealing compound for a variety of applications. For example, its extreme resistance to chemical and thermal degradation and its p-type semiconducting characteristics have led to its use as a hole transport layer in organic

\* Corresponding author. Tel.: +886 3 5726111x31873; fax: +886 3 5724727.

E-mail address: [wtwhang@mail.NCTU.edu.tw](mailto:wtwhang@mail.NCTU.edu.tw) (W.-T. Whang).

light-emitting diodes (OLEDs) [13] and as an active layer in organic thin film transistors (OTFTs) [14]. In addition, the excellent photoconductive properties of CuPc enable its application in the photoconductive layers of photocopying machines and solar cells [15,16]. All of these applications are based, however, on the electrical characteristics of CuPc in the form of thin films. To our knowledge, there have been no previous reports describing the applications of CuPc as 1D structures. The planar macrocyclic structure and extended  $\pi$ -electron system of CuPc molecules suggested to us that they would be good candidates for forming 1D structures through intermolecular  $\pi$ - $\pi$  stacking interactions. In this study we prepared 1D CuPc nanofibers and evaluated their field emission characteristics. We have characterized these CuPc nanofibers using scanning electron microscopy (SEM), X-ray diffraction spectroscopy (XRD), and high-resolution transmission electron microscopy (HRTEM) techniques.

## 2. Experimental procedure

The CuPc films were grown through vacuum sublimation in a thermal coater at a base pressure of ca.  $3 \times 10^{-6}$  torr. Commercial powders of CuPc were sublimed onto various substrates, including Al, Ti, TiN, Au, and SiO<sub>2</sub>, from a heated crucible. The temperature of the crucible was ca. 100 °C; the corresponding deposition rate, determined using a quartz crystal microbalance, was 3 Å/s. To study the effect of the temperature on the film morphology, these substrates were maintained at 25, 100, 150 or 200 °C. Structural investigations were performed using a JEOL JSM-6500 F scanning electron microscope. Grazing incident X-ray diffraction was performed using a PHILIPS X'Pert Pro X-ray diffraction system equipped with a Cu-K $\alpha$  radiation source. Contact angles and surface energies were determined using a KRUSS GH-100 universal surface tester. The profiles and fine structures of the nanostructures were imaged and analyzed using a JEOL JEM-2010 F high-resolution transmission electron microscope equipped with an Oxford energy dispersive spectrometer. The field emission measurements were performed in a vacuum chamber (ca.  $10^{-6}$  torr) with a cylindrical copper electrode (diameter: 2.2 mm) positioned above the substrate surface at a distance of 75  $\mu$ m. A Keithley 237 instrument was used to measure the emission current of the CuPc nanofibers as a function of the sweep bias.

## 3. Results and discussions

The choice of film growth method and the crystalline properties and surface energies of the substrates have profound effects on the surface morphologies of coated organic thin films [17]. In most cases, the crystallinity of the substrate strongly affects the crystallinity of the deposited film. The surface energy of the substrate, which governs the mobility of the deposited molecules on that surface, determines the wetting ability of the coated film. Therefore, to determine the growth conditions necessary to prepare 1D CuPc nanostructures, we deposited CuPc molecules onto different substrates, namely Al, Au, Ti, TiN and SiO<sub>2</sub>, at various temperatures and used SEM to investigate their morphologies.

Fig. 1(a) and (b) present SEM images of CuPc films deposited at room temperature onto SiO<sub>2</sub> and Au substrates, respectively. Both images display contiguous granular crystals that possess smooth morphologies. The mean diameters of the granular crystals formed on the Au and SiO<sub>2</sub> substrate were both ca. 25 nm. Similar granular morphologies were exhibited for the films coated on the other substrates (Al, Ti and TiN), although with different crystallite sizes. When the substrates were heated above 100 °C, however, we observed totally different morphologies. Fig. 1(c) displays the in-plane island morphology of the CuPc layer on SiO<sub>2</sub>. In contrast, the layer deposited onto the Au substrate possessed an out-of-plane 1D nanofiber morphology (Fig. 1(d)). The CuPc packing morphologies on TiN were similar to those on the gold surface, whereas those on the Ti and Al substrates were a mixture of both kinds. The average length of the nanofibers formed on the gold substrate was ca. 500 nm, with their diameters falling in the range 15–50 nm. At a higher deposition temperature, but with the same process time, the CuPc nanofibers that formed were longer and had larger diameters, but their density was lower. Fig. 2 displays the various morphologies of the CuPc layers deposited at (a) room temperature and at (b) 100, (c) 150 and (d) 200 °C. For the CuPc nanofibers deposited on the Au surface at 150 °C, the average length increased to 1  $\mu$ m and the mean diameter expanded to 60 nm.

Contact angle measurements indicate that SiO<sub>2</sub> has a higher surface energy (50.7 mJ/m<sup>2</sup>) than does gold (39.4 mJ/m<sup>2</sup>), suggesting that the oxide substrate has a higher concentration of unsaturated surface bonds, which tend to adsorb molecules to lower the surface free energy. Therefore, it was

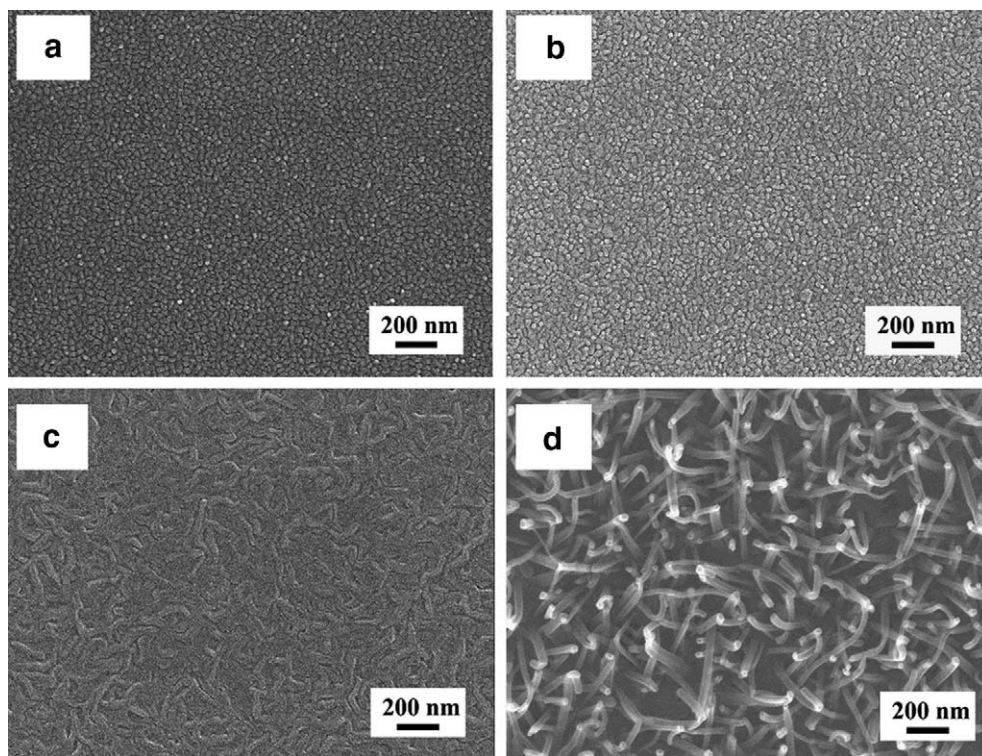


Fig. 1. Top-view SEM images of CuPc layers deposited at room temperature on (a) SiO<sub>2</sub> and (b) Au and at 100 °C on (c) SiO<sub>2</sub> and (d) Au.

not unexpected that the deposited CuPc molecules would have a stronger tendency to cover the whole SiO<sub>2</sub> surface, rather than stack to form out-of-plane nanofibers.

In the case of the CuPc layer formed on the gold substrate, the change in morphology that occurred upon increasing the temperature can be explained by considering the following equation [18]:

$$\gamma = \gamma^0 \left( 1 - \frac{T}{T_c} \right)^n \quad (1)$$

where  $\gamma$  is the surface energy at temperature  $T$  and  $\gamma^0$  is the surface energy at the critical temperature,  $T_c$ ; the value of  $n$  may be closer to unity for metals. According to this formula, the surface energy of the gold substrate decreases as the temperature increases. This reduction in surface energy weakens the molecule–substrate interactions, resulting in the intermolecular  $\pi$ – $\pi$  interactions becoming dominant. Meanwhile, the high substrate temperature favors surface diffusion, driving the adsorbed molecules toward growth at certain nucleation sites, which are formed owing to the lattice mismatch between CuPc and Au polycrystalline [19,20]. Therefore, the CuPc molecules prefer to stack up into

nanofibers, rather than spread out to cover the gold substrate in a mesh-like film.

The surface energies for Ti, Al and TiN are 37.51, 35.14 and 36.3 mJ/m<sup>2</sup>, respectively. These values are similar to – but lower than – the surface energy of the gold substrate. The CuPc layers on those substrates all exhibit the out-of-plane nanofiber morphology, except that a mesh-like morphology coexists on the Al and Ti substrates. Although the lower surface energies should lead to weaker interaction forces between the adsorbate and the substrates, these metal substrates are more easily oxidized than is the gold substrate. We suspect that the oxygen atoms of the resulting metal oxides react, or interact noncovalently, with the organic molecules to cause this phenomenon. For the TiN surface, its relative inertness toward oxygen and columnar crystal morphology combine to form the out-of-plane nanofiber structure.

Depending on its processing conditions, CuPc may form one, or a mixture, of many crystal phases, which are termed the  $\alpha$ ,  $\beta$ ,  $\gamma$ ,  $\delta$ ,  $\epsilon$ , and  $\chi$  phases [21]. Of the various polymorphic forms, the most common structures are the  $\alpha$  and  $\beta$  phases, which exhibit slightly different structural and electrical characteris-



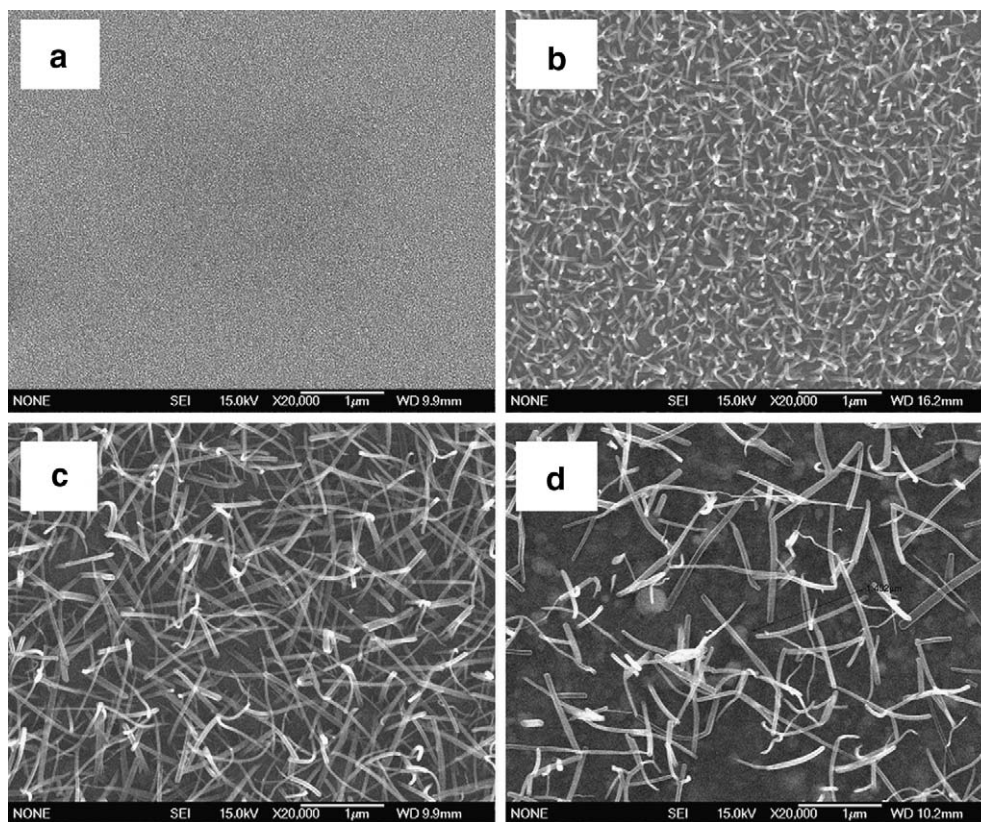


Fig. 2. Top-view SEM images of CuPc layers deposited on Au substrates at (a) room temperature and at (b) 100, (c) 150 and (d) 200 °C.

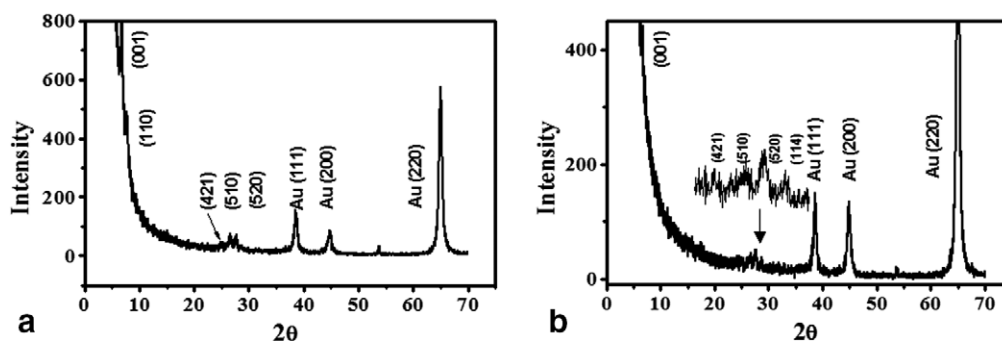


Fig. 3. XRD spectra of CuPc layers deposited on Au substrates at (a) room temperature and (b) 150 °C.

tics. Films deposited at room temperature exhibit the  $\alpha$  phase, whereas those deposited at higher-temperatures transform into the  $\beta$  phase [22]. Fig. 3(a) and (b) present the grazing incident X-ray diffraction (GID) patterns of the CuPc layers deposited at room temperature and 150 °C, respectively. The incident angle and the scan step used to obtain both patterns were 0.5° and 0.02°. The  $2\theta$  peaks at 38.4°, 44.7° and 64.9° in both patterns are associated with the gold substrate. The recognizable diffraction peaks of the

CuPc film at (001), (110), (4,2,1), (510), and (520) in Fig. 3(a) indicate that the CuPc film that we deposited at room temperature existed in the tetragonal  $\alpha$  phase [23]. The diffraction peaks from the CuPc nanofibers deposited at 150 °C (Fig. 3(b)) are similar to those arising from the CuPc film, but the (110) peak is absent. Although, in theory, the crystallinity of a film should be greater after higher-temperature processing, the morphology change (from a film to fibers) at the higher deposition temperature

resulted in a rough and discontinuous CuPc layer on the gold substrate, leading to lower intensities of some of the diffraction peaks. According to the reference diffraction peak for a monoclinic  $\beta$ -phase structure [23], at least three intense peaks should be present at  $7.0^\circ$ ,  $9.2^\circ$  and  $23.8^\circ$ . These peaks are absent in Fig. 3(b), suggesting that the structure of the CuPc nanofibers deposited at  $150^\circ\text{C}$  was that of the  $\alpha$  phase.

Fig. 4(a) presents an HRTEM image of a single CuPc nanofiber (diameter: 16 nm), which was synthesized on a heated gold substrate ( $100^\circ\text{C}$ ). Unlike related carbon nanotubes (CNTs), no catalyst appears at the top of the fiber. This feature was further verified after recording the energy dispersive spectra (EDS), which exhibited no peaks arising from gold atoms at any point along the entire length of the CuPc nanofiber. Fig. 4(b) presents a magnified image of the CuPc nanofiber; it exhibits fringes, suggesting that the CuPc units were stacked in the growth direction and aligned in a parallel manner. This high-resolution image indicates that the nanofibers formed through layered stacking of CuPc molecules. Fig. 4(b) also presents the corresponding profile analyzed using Fuji Imagegauge software. The average interlayer distance ( $4.3\text{ \AA}$ ) slightly exceeds the value of  $3.8\text{ \AA}$  found for the spacing  $h$  between two molecular layers along the stacking direction of  $\alpha$ -CuPc thin films [24], depicted schematically in Fig. 4(c). This difference may be caused

by the high aspect ratio of the 1D nanofiber structure, which suffers more stress and has a larger inclination angle ( $\varphi'$ ) of stacking than that angle ( $\varphi$ ) of 2D smooth thin film structures. Therefore, at a constant interlayer distance  $d$  ( $3.4\text{ \AA}$ ), a larger inclination angle ( $\varphi'$ ) corresponds to a greater distance  $h$ , according to the cosine relationship.

We performed field emission characterization of the CuPc nanofibers that we synthesized on a heated ( $100^\circ\text{C}$ ) gold substrate; this analysis was performed under vacuum ( $5 \times 10^{-6}$  torr) after placing a cylindrical Cu electrode (diameter: 2.2 mm)  $75\text{ }\mu\text{m}$  above the surface of the sample. The Cu electrode was connected to the source monitor unit (SMU) of a Keithley 237 instrument; the gold substrate under the CuPc nanofibers was grounded. Fig. 5 presents a plot of the emission current density  $J$  as a function of the applied field  $E$ . The turn-on field required for the CuPc nanofibers to produce a current density of  $10\text{ }\mu\text{A}/\text{cm}^2$  was  $13.6\text{ V}/\mu\text{m}$ , a value that is somewhat higher than the fields required for turning on other previously reported organic nanofibers [10–12]. The electron affinity ( $3.1\text{ eV}$ ) of CuPc [25] is much lower than the work function ( $5.1\text{ eV}$ ) of the gold substrate, so the energy barrier (ca.  $2\text{ eV}$ ) that exists at the metal–organic contact limits electron injection from the substrate. Consequently, the finite injected electrons require a higher electric field to reach the same level of emission current. The inset of Fig. 5 displays a plot of  $\ln(J/E^2)$  as a function of  $1/E$ ; this straight line

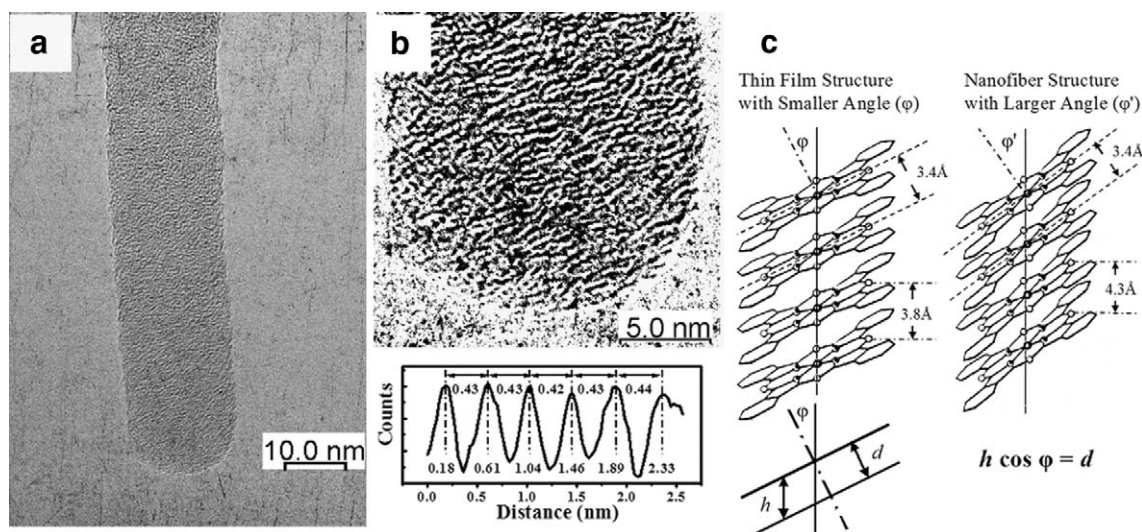


Fig. 4. (a) HRTEM image of a single CuPc nanofiber (diameter: 16 nm). (b) Magnified image of this nanofiber, which has been over-contrasted to intensify the fringes, and the corresponding profile analyzed using Fuji Imagegauge software. (c) Schematic illustration of CuPc molecules stacked at different inclination angles ( $\varphi$ ).

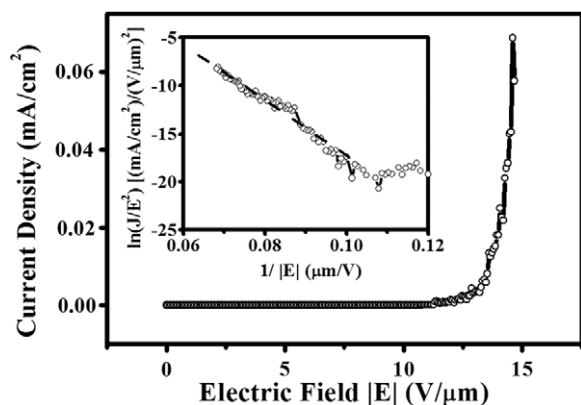


Fig. 5. Field emission  $J$ - $E$  curve of the CuPc nanofibers. Inset: Corresponding FN plot.

implies that the field emission from these nanofibers follows the Fowler–Nordheim (FN) theory [26–28]. Taking into account the work function of bulk CuPc (3.1 eV), we deduced the field enhancement factor  $\beta$  of the CuPc nanofibers from the slope of the FN plot to be ca. 130. Normally, the enhancement factor is proportional to the length-to-radius ratio ( $L/r$ ) of a 1D nanostructure [10]. Because the CuPc nanofibers reported herein possess shorter lengths (500 nm) and larger radii (50 nm), it is reasonable that they would exhibit a smaller enhancement factor relative to those of AlQ<sub>3</sub> organic nanowires [10]. Fig. 6 displays the emission current stability of the CuPc nanofibers when biased at 1000 V ( $E = 13.3$  V/ $\mu\text{m}$ ) for 1800 s. The mean current density was ca.  $3 \mu\text{A}/\text{cm}^2$ , with a perturbation within one order of magnitude, which may arise from the random orientation of the CuPc nanofibers on the surface. The field emission current did not decay during the period of the stability mea-

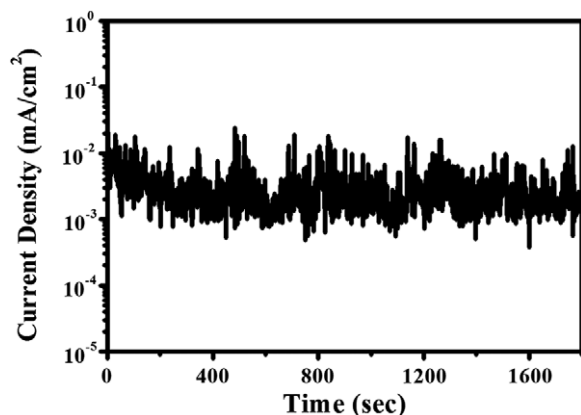


Fig. 6. Emission current stability of the CuPc nanofibers at constant voltage.

surement, suggesting that these CuPc organic nanofibers are suitable for use in electron emitting devices.

#### 4. Conclusions

In this paper, we describe a simple method for producing CuPc organic nanofibers at low-temperature. XRD analysis of these nanofibers revealed that they possessed  $\alpha$ -phase structures; HRTEM images indicated that they formed through layered stacking of CuPc molecules. The CuPc nanofibers exhibit field emission characteristics and follow Fowler–Nordheim behavior similar to that of CNTs. The stability of the emission current and the simplicity of the synthetic process suggest that these CuPc nanofibers may find a broad range of applications in nanoscience and nanotechnology.

#### Acknowledgments

We thank the National Science Council of the Republic of China for supporting this research financially under Contract No. NSC 94-2216-E-009-019. The technical support provided by the National Nano Device Laboratories is greatly appreciated. Authors also would like to thank Dr. Peter Glink for English correction.

#### References

- [1] W.A. de Heer, A. Châtelain, D. Ugarte, *Science* 270 (1995) 1179.
- [2] C.J. Lee, T.J. Lee, S.C. Lyu, Y. Zhang, H. Ruh, H.J. Lee, *Appl. Phys. Lett.* 81 (2002) 3648.
- [3] Z. Pan, H.L. Lai, F.C.K. Au, X. Duan, W. Zhou, W. Shi, N. Wang, C.S. Lee, N.B. Wong, S.T. Lee, S. Xie, *Adv. Mater.* 12 (2000) 1186.
- [4] J. Zhou, N.S. Xu, S.Z. Deng, J. Chen, J.C. She, Z.L. Wang, *Adv. Mater.* 21 (2003) 1835.
- [5] W. Yi, T. Jeong, S. Yu, J. Heo, C. Lee, J. Lee, W. Kim, J.B. Yoo, J. Kim, *Adv. Mater.* 20 (2002) 1464.
- [6] F.J.M. Hoeben, P. Jonkheijm, E.W. Meijer, A.P.H.J. Schenning, *Chem. Rev.* 105 (2005) 1491.
- [7] S.I. Stupp, V. LeBonheur, K. Walker, L.S. Li, K.E. Huggins, M. Keser, A. Amstutz, *Science* 276 (1997) 384.
- [8] H. Liu, Y. Li, S. Xiao, H. Gan, T. Jiu, H. Li, L. Jiang, D. Zhu, D. Yu, B. Xiang, Y. Chen, *J. Am. Chem. Soc.* 125 (2003) 10794.
- [9] J.P. Hill, W. Jin, A. Kosaka, T. Fukushima, H. Ichihara, T. Shimomura, K. Ito, T. Hashizume, N. Ishii, T. Aida, *Science* 304 (2004) 1481.
- [10] J.J. Chiu, C.C. Kei, T.P. Perng, W.S. Wang, *Adv. Mater.* 15 (2003) 1361.
- [11] S.C. Suen, W.T. Whang, B.W. Wu, Y.F. Lai, *Appl. Phys. Lett.* 84 (2004) 3157.

- [12] H. Liu, Q. Zhao, Y. Li, Y. Liu, F. Lu, J. Zhuang, S. Wang, L. Jiang, D. Zhu, D. Yu, L. Chi, *J. Am. Chem. Soc.* 127 (2005) 1120.
- [13] S.T. Lee, Y.M. Wang, X.Y. Hou, C.W. Tang, *Appl. Phys. Lett.* 74 (1999) 670.
- [14] Z. Bao, A.J. Lovinger, A. Dodabalapur, *Appl. Phys. Lett.* 69 (1996) 3066.
- [15] I.A. Levitsky, W.B. Euler, N. Tokranova, B. Xu, J. Castracane, *Appl. Phys. Lett.* 85 (2004) 6245.
- [16] P. Peumans, A. Yakimov, S.R. Forrest, *J. Appl. Phys.* 93 (2003) 3693.
- [17] F. Schreiber, *Phys. Status Solidi* 201 (2004) 1037.
- [18] A.W. Adamson, *Physical Chemistry of Surfaces*, John Wiley & Sons Publishers, 1990, p. 55.
- [19] F. Yang, M. Shtein, S.R. Forrest, *J. Appl. Phys.* 98 (2005) 014906.
- [20] Y.L. Lee, W.C. Tasi, J.R. Maa, *Appl. Surf. Sci.* 173 (2001) 352.
- [21] H. Saijo, T. Kobayashi, N. Uyeda, *J. Cryst. Growth* 40 (1997) 118.
- [22] T.V. Basova, B.A. Kolesov, *Thin Solid Films* 325 (1998) 140.
- [23] 2001 JCPDS-International Centre for Diffraction Data; (a) PDF No. 06-0007 for  $\alpha$ -CuPc, (b) PDF No. 37-1846 for  $\beta$ -CuPc.
- [24] R. Hiesgen, M. Rabisch, H. Böttcher, D. Meissner, *Sol. Energy Mater. Sol. Cells* 61 (2000) 73.
- [25] A.K. Mahapatro, S. Ghosh, *Appl. Phys. Lett.* 80 (2002) 4840.
- [26] R.H. Fowler, L. Nordheim, *Proc. R. Soc. London, Ser. A* 119 (1928) 626.
- [27] R.D. Young, *Phys. Rev.* 113 (1950) 110.
- [28] A. Buldum, J.P. Lu, *Phys. Rev. Lett.* 91 (2003) 236801.